Canadian Acoustics / Acoustique Canadienne 25(4) 3-11 (1997) ***Research article / Article de recherche***

COMPARISON OF SOME METHODS USED FOR PREDICTION OF ATMOSPHERIC SOUND PROPAGATION

Marta Galindo*, Michael R. Stinson and Gilles Daigle

Institute for Microstructural Sciences
National Research Council
Ottawa, Ontario K1A 0R6, Canada

ABSTRACT

The sound field in inhomogeneous atmospheric conditions above an impedance plane is computed using three different numerical procedures, to assess their advantages and disadvantages. Two implementations of the parabolic equation are considered, the Green's function method and a Crank-Nicolson method; these are contrasted with a version of the fast field program. As test cases, both upward and downward refracting conditions are considered, with and without turbulence. Calculations made using the Green's function implementation are considerably faster, making it the method of choice when large numbers of calculations (as when many realizations of turbulence are required) are necessary. However, considerable care is required in setting computational parameters and parallel calculations with one of the other techniques for validation is advisable.

SOMMAIRE

Le champ sonore en présence d'un plan d'impédance est calculé à partir de trois méthodes numériques différentes afin d'évaluer leurs avantages et désavantages. On compare deux applications de l'équation parabolique; une méthode basée sur la fonction de Green et une méthode Crank-Nicolson. Ces deux méthodes sont aussi comparées avec une version du Fast Field Program. On traite les cas de la propagation en présence d'un gradient de célérité négatif et d'un gradient de célérité positif, en présence de turbulence et sans turbulence. La méthode basées sur la fonction de Green s'avère la plus rapide, ce qui lui donne une avantage lorsque le nombre de calcul est grand (en présence de turbulence, le calcul doit être effectué pour un nombre important de réalisation du champ turbulent). Cependant, un soin particulier doit être apporté au choix des paramètres de calcul et des calculs parallèles en utilisant une des autres méthodes sont souhaitables pour valider les resultats.

*On a work term from the Danish Technical University

1. INTRODUCTION

With the ever-increasing speed of computers and the development of more efficient numerical algorithms, it is becoming possible to obtain quite realistic predictions of sound fields in the atmosphere.[1,2] The important physical mechanisms that control propagation, e.g., turbulence, refraction and terrain, can be examined directly and modelled more rigorously.[3,4] Ultimately, the knowledge generated will find its way into standards and regulatory prediction schemes. Three current approaches for the numerical computation of atmospheric sound propagation will be discussed and contrasted in this paper.

Many physical factors influence sound propagation.[5,6] The ground over which propagation occurs is rarely flat and interacts with the sound field through its ground impedance. The atmosphere is neither homogeneous nor static. The average sound speed generally varies with height above ground, giving rise to upward or downward refrac-

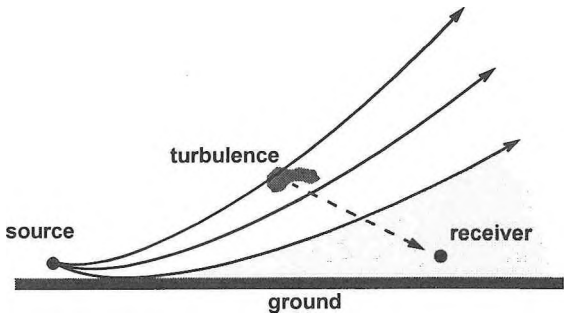

Figure 1. Sketch showing upward refraction conditions. The sound speed decreases with height, causing sound rays to curve upwards. In the acoustic shadow, the sound field is dominated by scattering from atmospheric turbulence.

tion conditions. Local inhomogeneities of wind speed or temperature or humidity, i.e., turbulence, will scatter sound energy. A typical situation found on warm summer afternoons is shown in Fig. 1. Because of solar heating, the air nearer the ground is warmer and the sound speed is greater there than higher up. Sound rays will tend to curve up, forming an acoustic shadow. Within the shadow, measured sound pressure levels are much higher[7] than would be predicted on the basis of simple theory. It is generally accepted that scattering of sound by turbulence is the dominant source of acoustic energy within such a shadow.

A useful survey of models currently being used for sound field computation may be found in the Benchmark paper[4]: ray-based methods, parabolic equation techniques and "fast field program" implementations are discussed. The latter two classes of methods are particularly useful, giving comparable accuracy and handling a wide range of sound speed profiles. Of these two classes, only those based on a solution of the parabolic equation have been proven able to handle turbulence in a realistic fashion. Two implementations of the parabolic equation, one based on a Crank-Nicolson finite-difference scheme[8] and the other, the "Green's function" parabolic equation, on a split-step Fourier implementation that explicitly treats the ground impedance condition,[9,10] are discussed in this paper. These typify the two main approaches to solution of the parabolic equation. The fast field program, although not able to treat turbulence directly, is a robust and accurate procedure[11,12] and provides a useful verification of the parabolic equation approaches.

Gilbert and Di have found that the Crank-Nicolson and Green's function approaches give comparable results for the no-turbulence case[9] and qualitatively similar results with turbulence.[10] This comparison will be explored further here.

Other implementations of the parabolic equation have been discussed, particularly in the underwater acoustics forum.[13,14] Many of these approaches, however, have been tailored for the underwater environment, where the bottom is treated differently than an impedance condition and turbulence is not generally important. A recent development, the split-step Padé approximation[15] could prove to be quite useful in atmospheric acoustics and an initial implementation by Juvé *et al.*[2] is promising.

2. THEORY

The relevant theory does appear elsewhere and so will only be covered briefly here.

Consider a point acoustical source located a height z_s above an impedance plane. For a harmonic time dependence $\exp(-i\omega t)$, the complex sound pressure p is given by the wave equation

$$[\nabla^2 + k^2]\, p(x, y, z) = -4\pi\delta(x, y, z - z_s) \qquad (1)$$

where $k = \omega/c$ is the wavenumber. Because of turbulence in the atmosphere and the formation of refractive profiles, the sound speed varies with spatial position and, hence, so does the wavenumber. We restrict our attention to a vertical plane containing source and receiver, so only the horizontal range r and height z above the ground need be considered. It is convenient, then, to separate the wavenumber into two components,[1] a deterministic component $k_d(z)$ due to the static refractive profile, and a stochastic component $k_o\mu(r, z)$, through

$$k(r, z) = k_d(z) + k_o\mu(r, z)\ , \qquad (2)$$

where k_o is a reference value. The impedance boundary condition for a specific surface impedance Z, is

$$\left(\frac{\partial p}{\partial z} + ik\beta p\right)_{z=0} = 0\ , \qquad (3)$$

with $\beta = \rho c/Z$ being the complex surface admittance.

Expressing Eq. (1) in cylindrical coordinates and assuming symmetry about the vertical axis passing through the source, we obtain

$$\frac{\partial^2 p}{\partial r^2} + \frac{1}{r}\frac{\partial p}{\partial r} + \frac{\partial^2 p}{\partial z^2} + k^2 p = -\frac{2}{r}\delta(r)\delta(z - z_s)\ , \qquad (4)$$

where r is the horizontal distance from source. This is the point of departure for the fast field program (FFP) and the parabolic equation (PE) approaches.

2.1. Fast Field Program

In the fast field program (FFP), the atmosphere is treated as horizontal layers and turbulence is explicitly omitted, so $\mu = 0$ in Eq. (2). The range dependence is removed from Eq. (4) by applying the Hankel transform to give

$$\frac{d^2P}{dz^2} + [k^2(z) - K^2]P = -2\delta(z - z_s) \tag{5}$$

where the transform P is

$$P(K, z) = \int_0^\infty p(r, z) J_0(Kr) r dr . \tag{6}$$

Equation (5) presents a one-dimensional problem. Solutions are relatively straightforward[4,16,17] although details of implementation (e.g., whether sound speed is assumed constant or linearly-varying within each layer) lead to different versions of the fast field program. Given a solution $P(K, z)$ for each horizontal wavenumber K, the range dependence of the sound field is obtained by applying the inverse Hankel transform,

$$p(r, z) = \int_0^\infty P(K, z) J_0(Kr) K dK . \tag{7}$$

The integral can be replaced by a finite sum of N terms (discretizing both range r and wavenumber K) more suitable for computation, making use of the asymptotic form for the Bessel function,[16]

$$p(r_m) = 2e^{i\pi/4} \sqrt{\frac{\pi}{r_m}} \Delta K \sum_{n=0}^{N-1} P(K_n) \sqrt{K_n} e^{i2\pi mn/N}, \tag{8}$$

at each height z. This form is able to take advantage of fast Fourier transform techniques.

2.2. Crank-Nicolson PE

To obtain the parabolic equation, the substitution $U = pr^{1/2}$ and the far-field assumption $kr \gg 1$ are made in Eq. (4), giving

$$\frac{\partial^2 U}{\partial r^2} + \frac{\partial^2 U}{\partial z^2} + k^2 U = 0 . \tag{9}$$

An operator $Q = k^2 + \partial^2/\partial z^2$ is introduced and Eq. (9) is factored into

$$\left(\frac{\partial}{\partial r} + i\sqrt{Q}\right)\left(\frac{\partial}{\partial r} - i\sqrt{Q}\right) U = 0 ; \tag{10}$$

the two factors correspond to outgoing and incoming waves. (Strictly, this factorization is an approximation and holds exactly only when the operator Q is range-independent.) In many cases backscattering can be ignored so only the outgoing wave is retained, i.e.,

$$\frac{\partial U}{\partial r} = i\sqrt{Q} U . \tag{11}$$

For the Crank-Nicolson approach, this *one-way equation* is numerically solved using a finite difference approach. In our implementation,[8] the operator $\sqrt{Q}$ is approximated using Claerbout's rational Padé expansion[18]

$$\sqrt{Q} \equiv k_o \sqrt{1 + q} \approx k_o \frac{1 + 3q/4}{1 + q/4} , \tag{12}$$

where for a reference wavenumber k_o and an index of refraction $n = k/k_o$,

$$q = (n^2 - 1) + \frac{1}{k_o^2} \frac{\partial^2}{\partial z^2} . \tag{13}$$

From Eq. (2), the index of refraction contains deterministic and stochastic components according to

$$n(r, z) = n_d(r, z) + \mu(r, z) . \tag{14}$$

Assuming weak turbulence, $\mu^2 \ll 1$, the operator q can be written as[19]

$$q = q_d + 2\mu n_d , \tag{15}$$

where

$$q_d = n_d^2 + \frac{1}{k_o^2} \frac{\partial^2}{\partial z^2} - 1 , \tag{16}$$

so a separation of deterministic and stochastic components has been effected. The range dependence is treated through a finite difference approach and the vertical dependence, through a linear finite element approach[20], leading to a matrix equation: With the $U(r, z_n)$ at heights z_n being the elements of the vector $V(r)$, the resulting system of equations have the form

$$\mathrm{M}^- V(r + \Delta r) = \mathrm{M}^+ V(r) , \tag{17}$$

where the matrices M^- and M^+ are tridiagonal. Given $V(r)$ at one range step, the field $V(r + \Delta r)$ at the next range step is obtained using a Gaussian decomposition procedure. The boundary condition, also discretized, is applied as a constraint on the lowest z_n above the ground. The recalculation of the stochastic matrix at each range step

increases computation time significantly over the simply deterministic case. It is not possible to use a *split-step Fourier* technique (discussed next section) which would reduce computation time.

2.3. Green's Function PE

A faster implementation of the parabolic equation is the Green's function PE, developed by Gilbert and Di[9,10] for atmospheric propagation. This work is based on the *split-step Fourier* technique developed for underwater acoustics[13] but directly incorporates the impedance boundary condition. The approximations that go into this approach have been discussed by Havelock *et al.*[21] Equation (11) is integrated formally to give

$$U(r+\Delta r, z) = e^{ik\sqrt{Q}\Delta r} U(r, z) \ . \tag{18}$$

In applying the *split step* approximation, the operator Q is first written as

$$Q = Q_o + \delta k^2 + 2k_o k_d \mu \tag{19}$$

where $Q_o = k_o^2 + \partial^2/\partial z^2$, $\delta k^2 = k_d^2 - k_o^2$, k_o is a reference wavenumber and a term in μ^2 has been ignored. With these, it is found that Eq. (18) can be written

$$U(r+\Delta r, z) \approx e^{i\Phi} e^{i\delta k^2 \Delta r/2k_o} e^{ik\sqrt{Q_o}\Delta r} U(r, z) \ . \tag{20}$$

Now, terms involving deterministic and stochastic, range-dependent and range independent have been separated. The effects due to turbulence are entirely within the first *phase screen* term, with the change in acoustic phase across Δr being given by

$$\Phi(z) = k_o \int_{\Delta r} \mu(r, z)\, dr \ . \tag{21}$$

The effects due to the sound speed profile are contained within the second term of Eq. (20). Both these terms are simple multiplicative factors. The third term is evaluated further using a spectral decomposition approach, leading to a Fourier transform formulation that directly accounts for the ground impedance. FFT techniques may be used to permit rapid evaluation of this term.

As with the Crank-Nicolson approach, a marching solution is implemented. However, the range step can be much larger with the Green's function PE, leading directly to more rapid computation.

3. COMPARISON PROCEDURE

3.1. Test cases

The three techniques discussed above will be compared using four specific scenarios, upward and downward refraction conditions, with and without turbulence. All three techniques treat propagation for a single frequency component; a sound frequency of 500 Hz was selected because of its importance in many noise propagation situations. Flat grassland, with a ground impedance of $Z/\rho c = (5.57, 6.1)$, was considered. The source is 1.5 m above the ground and the receiver is 2 m above the ground.

A logarithmic sound speed profile[1]

$$c_d(z) = \begin{cases} c_o + a\ln(z/d) \ , & z \geq z_o \\ c_o + a\ln(z_o/d) \ , & z < z_o \end{cases} \tag{22}$$

is used, with values of c_o=340 m/s, d=0.006 m, and z_o=0.05 m. For downward refraction, a value of a=2 m/s is used and for upward refraction, a=-2 m/s. The two profiles are shown in Fig. 2.

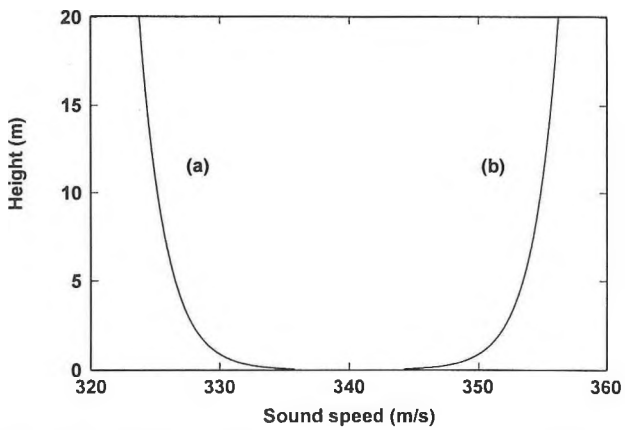

Figure 2. The sound speed profiles that will be used in the following comparisons showing (a) an upwardly refracting profile and (b) a downwardly refracting profile.

Each realization of a turbulent structure $\mu(r, z)$ in the atmosphere is generated using a Fourier approach.[1] For turbulence wavenumbers κ_r and κ_z corresponding to variations of μ in the r and z directions, respectively, we take

$$\mu(r, z) = \sum_{\kappa_r, \kappa_z} G(\kappa_r, \kappa_z) e^{-i\kappa_r r} e^{-i\kappa_r z} \ . \tag{23}$$

The μ are specified on a grid of points in the r-z plane, as $r = m\delta r$ and $z = n\delta z$, where $m=0,1,...(M-1)$ and $n=0,1,...(N-1)$. Correspondingly, the wavenumbers κ_r and κ_z have spacings of $\delta\kappa_r = 2\pi/M\delta r$ and $\delta\kappa_z = 2\pi/N\delta z$. The simulations used a grid spacing of $\delta r = \delta z = 0.05$ m (this choice is discussed further in the next section).

Each set of the complex Fourier coefficients $G(\kappa_r,\kappa_z)$ corresponds to a different realization or "snapshot" of a turbulent atmosphere. The phase angles of these coefficients are assigned randomly. The magnitudes, though, are assigned according to the spectral model being assumed. Consider the spatial correlation function defined as

$$C(s_r,s_z) = \langle \mu(r,z)\, \mu(r+s_r, z+s_z) \rangle , \tag{24}$$

where the triangular braces indicate spatial averaging over the displacement (s_r, s_z). It can be shown that the magnitude of $G(\kappa_r,\kappa_z)$ is related to the Fourier transform of $C(s_r, s_z)$ according to[1]

$$\left|G(\kappa_r, \kappa_z)\right|^2 = \frac{1}{MN}\sum_{r,z} C(s_r, s_z) e^{i\kappa_r r} e^{i\kappa_z z} . \tag{25}$$

Chernov[22] suggested that the measured correlation function is given approximately by

$$C(s_r, s_z) = \langle \mu^2 \rangle e^{-(s_r^2 + s_z^2)/L^2} , \tag{26}$$

where $\langle \mu^2 \rangle$ is the mean square strength of the fluctuations and L is a measured spatial correlation length. Daigle[23] found that measured spectra were approximately of this form. Substituting this function into Eq. (25) and evaluating the sums, we obtain to a very good approximation the Gaussian power spectrum

$$\left|G(\kappa_r,\kappa_z)\right|^2 = \frac{\langle \mu^2 \rangle \pi L^2}{MN\delta r \delta z} e^{-(\kappa_r^2 + \kappa_z^2)L^2/4} . \tag{27}$$

For the simulations, a correlation length of 1.1 m and a mean square fluctuation of $\langle \mu^2 \rangle = 2 \times 10^{-6}$, consistent with typical measurements, were assumed. Because of memory constraints in the code of the Crank-Nicolson PE approach, we were limited to $M=N=512$. The final turbulence structure (25.6 m a side) was then repeated throughout the r-z plane. For the Green's function PE, phase screens were computed using Eq. (21) over range steps of $\Delta r = 6.4$ m.

3.2. Implementation issues

All three techniques require some care in their implementation.

We are using the CERL version[11,12] of the fast field program. Only the number and distribution of sound speed layers and the number of integration points were varied. Default values for other parameters (K_{max}, extra loss) were used while the number of points per FFT was usually 2048. It is important to have sufficient layering to represent the sound speed profile and sufficient number of sampling points to represent the integrand of Eq. (7). The position of the layers was calculated using a simple power law of the form $z = 10^{-1.4 + n\Delta x}$ (with n=0,1,...) and convergence was achieved for $\Delta x \sim 0.01$.

The parabolic equation approaches require that the vertical grid size be small compared to a wavelength. A step of $\delta z = 0.05$ m was used (generally, a step of 1/5 wavelength is acceptable). The Green's function approach, using a total vertical height of 819.2 m, thus contained 16384 grid points and a FFT (and inverse FFT) of that size was required at each range step. The Crank-Nicolson approach used 12000 grid points.

The horizontal range step, for the Crank-Nicolson approach, must also be small; a step of $\delta r = 0.05$ m was used in these calculations to be consistent with the specification of the turbulence (ordinarily, a step of 1/5 wavelength would be used). The Green's function approach permits a much larger range step and, in the calculations to follow, a step of 6.4 m was used. In fact, using too small of a range step with this technique leads to numerical difficulties[24] (due to an increased importance of evanescent contributions to the sound field) and the smaller range step must be compensated by both a reduced δz and an increased vertical range.

The two PE approaches require specification of the vertical sound pressure distribution at the first range step; the best starting field available in the current codes was used for each. The Green's function PE approach used a Gaussian starting field[9]. The Crank-Nicolson implementation made use of a "Back PE" technique[19,25] to generate its starting field. The truncation of the vertical grid at the desired upper height leads to a false reflection of sound energy back toward the ground. To reduce this reflection and restore the radiation boundary condition, an artificial absorbing layer is introduced. In this layer, an imaginary part is added to the index of refraction function n^2, increasing gradually from a zero value at the start of the absorbing layer.[9] The absorbing layer was introduced at a height of about 250 m above ground for both approaches.

For the Green's function PE, the reference sound speed must be chosen carefully to get agreement with the other techniques. A value of 330 m/s was used for the upward refraction case and a value of 352 m/s, for the downward refraction case.

4. RESULTS

The calculated sound pressure level, for each case, will be presented as a function of horizontal range for a single receiver height of 2 m. The curves are normalized by the free field levels that would be obtained in the absence of ground, refractive profiles and turbulence, i.e., they are relative to free field.

4.1. Downward refraction, no turbulence

The relative sound pressure level as a function of range is shown in Figure 3, for the case of downward refraction with no turbulence. The three curves correspond to calculations using the Crank-Nicolson PE, the Green's function PE and the fast field program. Very good agreement is obtained between the three methods. On average, the relative levels are about constant with range, indicating that the additional energy refracted toward the ground is tending to compensate for attenuation by the ground. The various dips show the regions of constructive and destructive interference typical of downward refraction. The Green's function PE prediction is approximately 1 dB higher than the other two predictions, in part because of the choice of a Gaussian starter field[19].

Considerable differences between methods are found in speed of computation and ease of implementation. The times required to generate the curves of Fig. 3 on a 486-class computer using the Green's function PE, the fast field program, and the Crank-Nicolson PE were approximately 2 min., 5 min., and 20 min., respectively. It should be noted, though, that this comparison is appropriate only if the sound pressure level is required at just a single height. If the sound field is required over a two-dimensional region of the *r-z* plane (not an unusual situation), then the fast field program (i.e., our implementation) must be rerun for each height desired. The two PE methods, by virtue of the marching technique of the algorithms, actually generate solutions at all heights simultaneously so no additional computation time is required. For example, if the sound field was to be determined at 50 or more vertical positions over the same horizontal range as shown in Fig. 3, then the computation time using the fast field program would increase to something like 4 hours, considerably more than the Crank-Nicolson PE approach. It is noted, though, that there are SAFARI implementations[29] of the fast field program that are able to handle multiple receiver positions without an undue increase in computation time.

On the other, the Green's function PE required considerably more care in implementation than the other techniques. Calculations were repeated using different values of the key parameters (e.g., $k_o.\delta r$, δz and maximum z) to ensure that stable and convergent solutions had been obtained. The Crank-Nicolson PE approach tended to require the least "tuning".

4.2. Downward refraction, with turbulence

In Fig. 4, the two parabolic equation approaches are compared for the case of downward refraction with a superimposed turbulence structure. The fast field program is unable to handle atmospheric turbulence. It is important to note that the inclusion of turbulence does *not* significantly slow down the calculation using the Green's function approach. However, calculations made using the Crank-Nicolson PE method require much more computation time when turbulence is included (more than 12 hours using a 486-class computer were required to compute the curve in

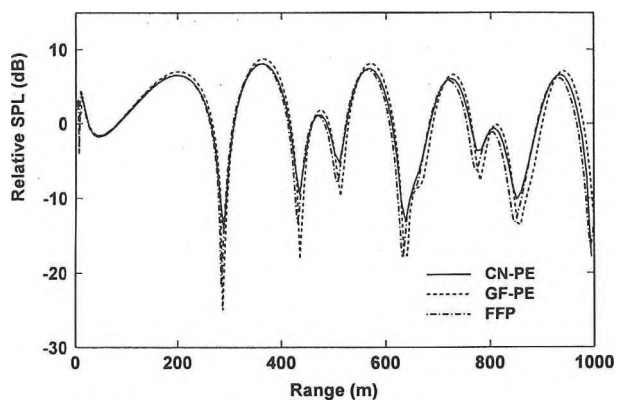

Figure 3. Downward refraction, no turbulence. The three curves are obtained using the Crank-Nicolson (CN-PE) and Green's Function (GF-PE) implementations of the parabolic equation and the fast field program (FFP).

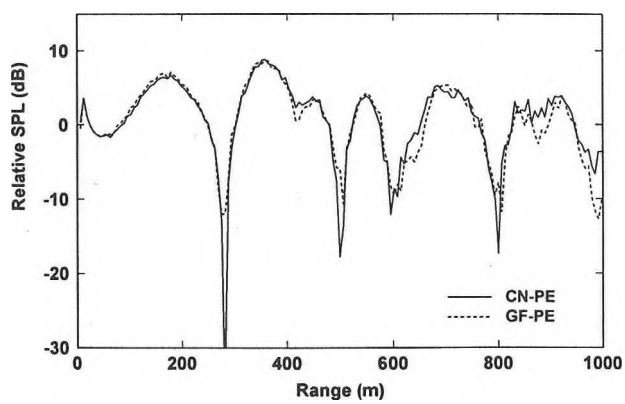

Figure 4. Downward refraction, with turbulence present. Predictions of the Crank-Nicolson (CN-PE) and Green's function (GF-PE) versions of the parabolic equation are shown.

Fig. 4). This slowdown is a result of having to recalculate the stochastic matrix at each range step.

The effect of including turbulence, seen by comparing Figs. 3 and 4, is evident but is relatively small in the downward refracting condition because this is "line-of-sight" propagation. The two methods of calculation are in reasonable agreement in that they modify the corresponding curves of Fig. 3 in a similar fashion.

It should be noted the calculations shown here correspond to a single "snapshot" of turbulence in the atmosphere. For a comparison to real measurements, many such realizations of a turbulent atmosphere would have to be generated and energy-averaged to give the equivalent rms levels that would be obtained experimentally.

4.3. Upward refraction, no turbulence

The results for an upwardly-refracting sound speed profile, i.e., the profile in Fig. 2(a), with no turbulence, are shown in Fig. 5. All three computational techniques are included. The relative levels drop rapidly with range (this is the acoustic shadow), falling to -50 dB for a range of 150 m. For ranges greater than 150 m or so, for this scenario, numerical noise was found to limit the calculations for all three techniques.

There are no significant differences between the predictions of the three approaches. The computational times are the same for upward refraction as for the downward refraction case.

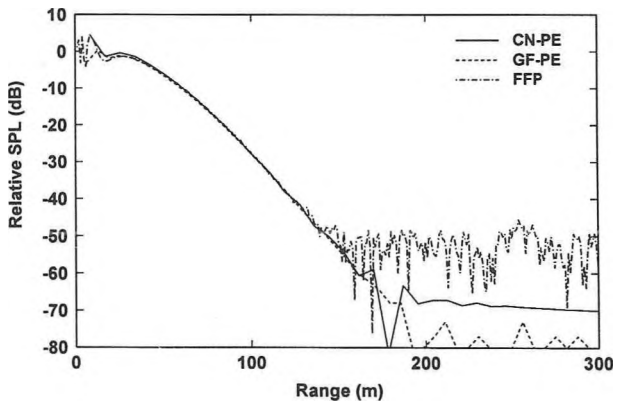

Figure 5. Upward refraction, no turbulence. The same three numerical approaches used in Figure 3 are applied here.

4.4. Upward refraction, with turbulence

In Fig. 6, the predictions for the two implementations of the parabolic equation are shown for an upwardly refracting atmosphere with turbulence. The importance of turbulent scattering is immediately apparent when this figure is compared to Fig. 5 which did not include turbulence. The relative sound pressure level does not decrease rapidly with range but levels off at about -30 dB, consistent with observations.[7]

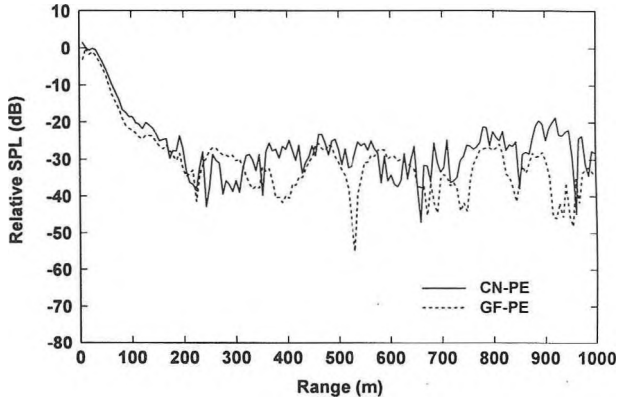

Figure 6. Upward refraction with a single realization of turbulence, showing the Crank-Nicolson and Green's function implementations of the parabolic equation.

The two predictions are qualitatively similar, levelling off to about the same value at large ranges. The curve for the Green's function PE prediction is smoother, as would be expected since it uses a larger range step. There are significant differences in the fine structure of the curves, though. The Crank-Nicolson PE used here employs a "wider-angle" approximation for the propagation operator $\sqrt{Q}$ than does the Green's function PE implementation,[9] so larger-angle scattering by turbulence may be treated more accurately. The correlation length of 1.1 m that has been assumed for the Gaussian turbulence spectrum means that there will be significant spatial variations of sound speed over distances as small as a meter or so. Additonal calculations are required to determine how well the Green's function PE accommodates structures of a size less than the range step.

These calculations correspond to a single realization of the turbulence, i.e., propagation through a frozen turbulent structure. The actual atmosphere is not static but constantly evolving in time and measured sound pressure levels are rms averages. To calculate corresponding levels, it is necessary to repeat the calculations many times, using a different turbulence realization with each. For enough realizations, the energy-average of the predictions will correspond to the rms level that would be measured.[26,27] Using the Green's function PE, with the same refractive profile and statistical description of turbulence as for Fig. 6, the mean relative sound pressure level as a function of

range is found to be as shown in Fig. 7. A total of 200 realizations were used in this averaging, giving an uncertainty of less than 0.5 dB.

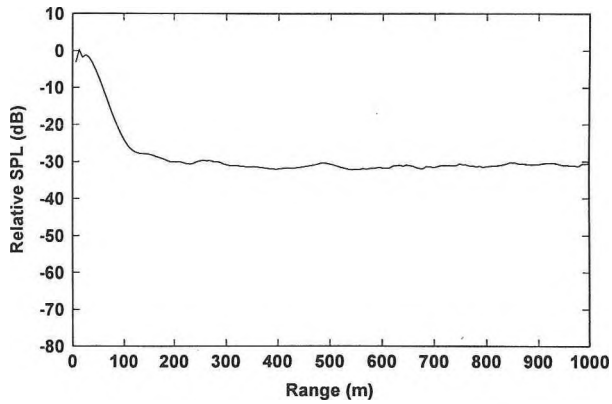

Figure 7. Upward refraction, with turbulence. Calculations for 200 different realizations of a turbulent atmosphere have been energy-averaged. The Green's function PE method has been used.

5. DISCUSSION

Overall, the different methods of calculation are in quite good agreement. Without turbulence, the fast field program and the two parabolic equation approaches gave very similar predictions. With turbulence present, there are differences in detail between the two parabolic equation predictions (i.e., the Crank-Nicolson and the Green's function PE) but the agreement is still reasonble and the key features are produced by both.

Computational speed is an important issue when realistic predictions of sound fields in the atmosphere, with turbulence included, are desired. Typically, 100-200 such realizations are required for each frequency or geometry chosen.

The fast field program works very well, in the absence of turbulence. It serves as a benchmark technique by which others can be tested for accuracy. The main drawback of this technique is its inability to handle turbulence which, as seen in comparing Figs. 5 and 6, is a very important factor in atmospheric propagation. Raspet[28] has done some work on incorporating turbulence into the fast field program, but the approach is somewhat indirect. The other disadvantage of this technique is the slow calculation speed, particularly when sound fields at many heights are required.

The Crank-Nicolson version of the parabolic equation method is straightforward to operate, requiring relatively little adjustment. It can handle turbulence and refractive profiles. However, the need for small range steps (typically $\lambda/5$) significantly limits its speed, particularly when turbulence is included in the description of the atmosphere.

The Green's function version of the parabolic equation is much faster[10], by a factor of 50-100. Its speed is a result of the relatively large range steps permitted (many wavelengths per step) and is achieved whether or not turbulence is included in the computation. However, this technique requires considerable care[24] in setting parameter values to ensure an accurate solution. For a selected range step, the vertical resolution must be sufficiently small and the number of vertical steps sufficiently large. Calculations are quite sensitive to the selection of reference sound speed c_o. As a result of its formulation, the technique has more difficulty with what would be considered simple cases (e.g., propagation above a rigid surface, in a homogenous atmosphere).

6. CONCLUSIONS

Three current methods for the calculation of sound fields above an impedance plane are discussed, the fast field program and the parabolic equation, with Crank-Nicolson and Green's function implementations. All are capable of generating accurate solutions. Only the parabolic equation methods have been shown to produce reliable predictions when turbulence is present in the atmosphere.

The Green's function PE is much faster computationally and, for this reason, is probably favoured when turbulence is included and a large number of realizations are required. However, this technique does require more care and fiddling to ensure accurate calculations. Rough guidelines for the selection of calculation parameters do exist.[9,24] It seems advisable, though, to use the Greens's function PE method in conjunction with one of the other approaches to verify that solutions are accurate.

Recent work using the split-step Padé approximation[15,2] suggests that a compromise been speed and ease of operation may be possible.

REFERENCES

1 K.E. Gilbert, R. Raspet and X. Di, "Calculation of turbulence effects in an upward-refracting atmosphere", J. Acoust. Soc. Am. **87**, 2428-2436 (1990).

2. D. Juvé, Ph. Blank-Benon and P. Chevret, "Sound propagation through a turbulent atmosphere: Influence of the turbulence model" in *Proceeding of the 6th International*

Symposium on Long Range Sound Propagation, Edited by D.I. Havelock and M.R. Stinson (Ottawa, Canada, 1994).

3. M.R. Stinson, D.I. Havelock and G.A. Daigle, "Simulation of scattering by turbulence into a shadow region using the GF-PE method" in *Proceeding of the 6th International Symposium on Long Range Sound Propagation*, Edited by D.I. Havelock and M.R. Stinson (Ottawa, Canada, 1994).

4. K. Attenborough, S. Taherzadeh, H.E. Bass, X. Di, R. Raspet, G.R. Becker, A. Güdeson, A. Chrestman, G.A. Daigle, A. L'Espérance, Y. Gabillet, K.E. Gilbert, Y.L. Li, M.J. White, P. Naz, J.M. Noble and H.A.J.M. van Hoof, "Benchmark cases for outdoor sound propagation models", J. Acoust. Soc. Am. **97**, 173-191 (1995).

5. G.A. Daigle, M.R. Stinson and D.I. Havelock, "Use of the PE method for predicting noise outdoors", in *Proceedings of InterNoise 96*, 561-566 (1996).

6. M.R. Stinson, G.A. Daigle and D.I. Havelock, "Factors affecting atmospheric sound propagation above an impedance plane", in Canadian Acoustics **24** (Proceedings Issue), 48 (1996).

7. F.M. Wiener and D.N. Keast,"Experimental study of the propagation of sound over ground", J. Acoust. Soc. Am. **67**, 318-326 (1980).

8. M. Galindo, "Application of the parabolic approximation method to sound propagation above ground with impedance variations", in *Proceeding of the 6th International Symposium on Long Range Sound Propagation*, Edited by D.I. Havelock and M.R. Stinson (Ottawa, Canada, 1994).

9. K.E. Gilbert and X. Di, "A fast Green's function method for one-way sound propagation in the atmosphere", J. Acoust. Soc. Am. **94**, 2343-2352 (1993).

10. X. Di and K.E. Gilbert, "The effect of turbulence and irregular terrain on outdoor sound propagation", in *Proceeding of the 6th International Symposium on Long Range Sound Propagation*, Edited by D.I. Havelock and M.R. Stinson (Ottawa, Canada, 1994).

11. R. Raspet, S.W. Lee, E. Kuester, D.C. Chang, W.F. Richards, R. Gilbert and N. Bong, "Fast-field program for a layered medium bounded by complex impedance surfaces", J. Acoust. Soc. Am. **77**, 345-352 (1985).

12. S.W. Lee, N. Bong, W.F. Richards and R. Raspet, "Impedance formulation of the fast field program for acoustic wave propagation in the atmosphere", J. Acoust. Soc. Am. **79**, 628-634 (1986).

13. F.D. Tappert, "The parabolic approximation method", in *Wave Propagation and Underwater Acoustics*, edited by J.B. Keller and J.S. Papadakis (Springer-Verlag, New York, 1977).

14. D.J. Thomson and N.R. Chapman, "A wide-angle split-step algorithm for the parabolic equation", J. Acoust. Soc. Am. **74**, 1848-1854 (1983).

15. M.D. Collins, "A split-step Padé solution for the parabolic equation method", J. Acoust. Soc. Am. **93**, 1736-1742 (1993).

16. S.J. Franke and G.W. Swenson, Jr., "A brief tutorial on the Fast Field Program (FFP) as applied to sound propagation in the air", Applied Acoustics **27**, 203-215 (1989).

17. D.J. Thomson and M.E. Mayfield, "An exact radiation condition for use with the *a posteriori* PE method", J. Comp. Acoust. **2**, 113-132 (1994).

18. J.F. Claerbout, *Fundamentals of Geophysical Data Processing*, McGraw-Hill, New York (1976).

19. M. Galindo Arranz, "The parabolic equation method for outdoor sound propagation", Ph.D. thesis, Department of Acoustic Technology, Technical University of Denmark, Report No. 68 (1996).

20. K.E. Gilbert and M.J. White, "Application of the parabolic equation to sound propagation in a refracting atmosphere", J. Acoust. Soc. Am. **85**, 630-637 (1989).

21. D.I. Havelock, X. Di, G.A. Daigle and M.R. Stinson, "Spatial coherence of a sound field in a refractive shadow: comparison of simulation and experiment", J. Acoust. Soc. Am. **98**, 2289-2302 (1995).

22. L.A. Chernov, *Wave Propagation in a Random Medium*, McGraw-Hill, New York (1960).

23. G.A. Daigle, "Effects of atmospheric turbulence on the interference of sound waves above a hard boundary", J. Acoust. Soc. Am. **64**, 622-630 (1978).

24. M.R. Dobry, R.P. Hansen and D.H. Marlin, "Sensitivity analysis of the Green's function parabolic equation model for atmospheric sound propagation", J. Acoust. Soc. Am. **96**, 3276(A) (1994).

25. M. Galindo, "Approximations in the PE method: Phase and level errors in a downward refracting atmosphere", in *Proceedings of the 7th International Symposium on Long Range Sound Propagation* (in press).

26. X. Di and G.A. Daigle, "Prediction of noise propagation during upward refraction above ground", in *Proceedings of InterNoise 94* (Yokohama, Japan, 1994).

27. M.R. Stinson, D.I. Havelock and G.A. Daigle, "Comparison of predicted and measured sound pressure levels within a refractive shadow in the presence of turbulence", in *Proceedings of InterNoise 95* (Newport Beach, USA, 1995).

28. R. Raspet and W. Wu, "Calculation of average turbulence effects on sound propagation based on the fast field program formulation", J. Acoust. Soc. Am. **97**, 147-153 (1995).

29. H. Schmidt, "SAFARI Seismo-acoustic fast field algorithm for range-independent environments", SACLANT Undersea Research Centre, San Batrolomeo, Italy, Report SR-113 (1988).

01dB Inc.

Symphonie

Dual Channel Real Time Measurement System

ALL-IN-ONE

- ✓ Dual Channel Real Time Frequency Analyser
- ✓ Enviromental Noise Analyser
- ✓ Building Acoustics Analyser
- ✓ Vibration Analyser
- ✓ Sound Intensity Analyser
- ✓ Sound Power ISO 9614
- ✓ Digital recorder
- ✓ Octave Analyser
- ✓ Psycho-Acoustics/Sound Quality
- ✓ Type 1 ANSI 1.4
- ✓ Digital Filtering Type 0-IEC 1260, ANSI 51.11

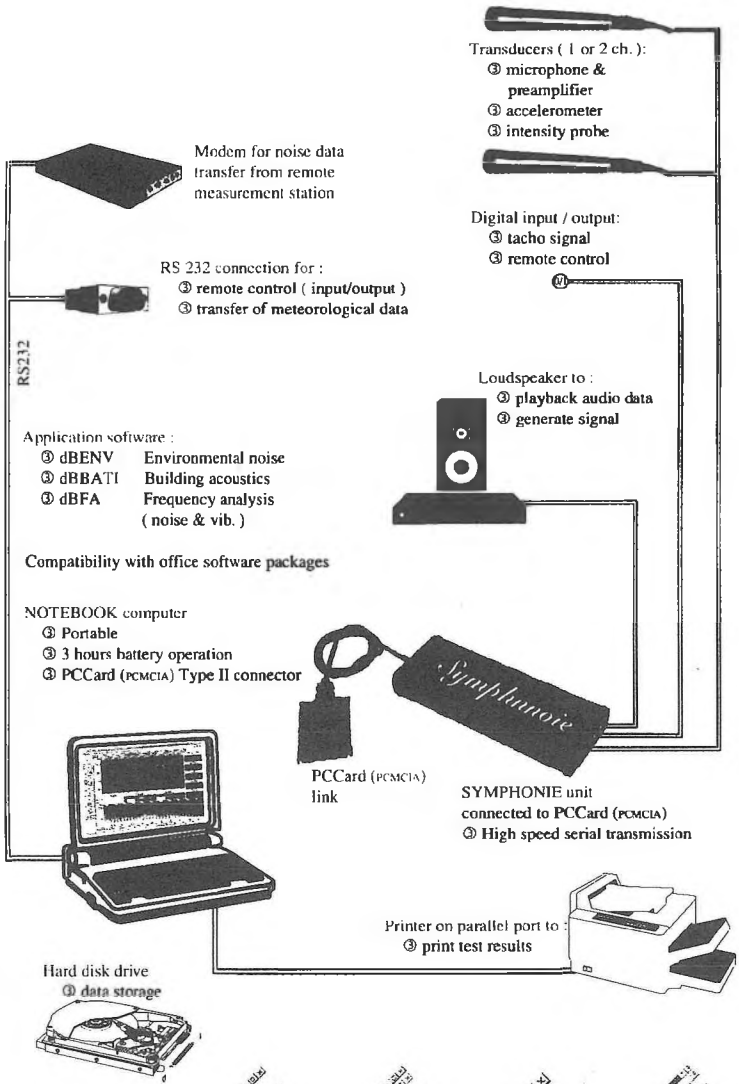

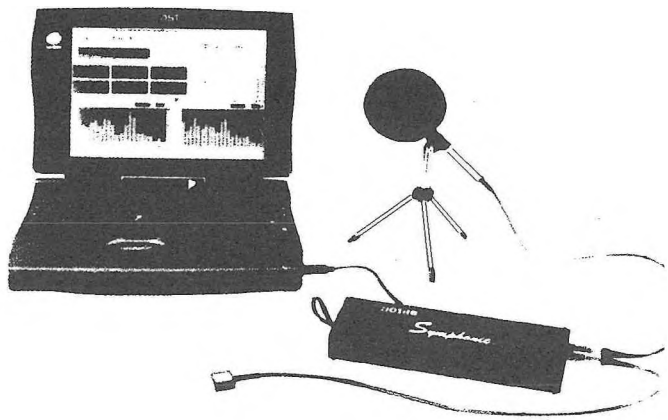

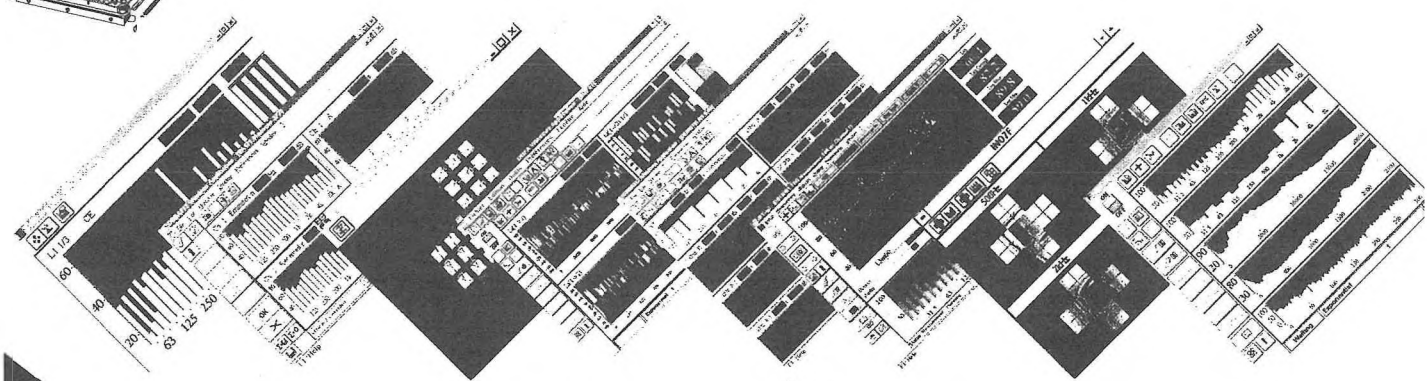

NOVEL DYNAMICS INC.
Dynamic Test and Analysis Systems

Toronto 519-853-4495 Fax 519-853-3366
Ottawa 613-599-6275 Fax 613-599-6274

Mediaacoustic
CD-ROM
Teaching Acoustics by Computer

MICROSOFT. WINDOWS. COMPATIBLE

Orders before Dec 22 receive Mediacoustic CD-ROM Free and 5 % discount on Gunnar Rasmussen Signature Series Microphones.